

Control of the collapse distance in atmospheric propagation

Gadi Fibich

School of Mathematical Sciences, Tel Aviv University, Tel Aviv, 69978 Israel

fibich@tau.ac.il

Yonatan Sivan

School of Physics and Astronomy, Tel Aviv University, Tel Aviv, 69978 Israel

Yosi Ehrlich, Einat Louzon, Moshe Fraenkel

NRC Soreq, Yavneh, 81800 Israel

Shmuel Eisenmann, Yiftach Katzir, Arie Zigler

Racah Institute of Physics, Hebrew University, Jerusalem, 91904 Israel

Abstract: We show experimentally for ultrashort laser pulses propagating in air, that the collapse/filamentation distance of intense laser pulses in the atmosphere can be extended and controlled with a simple double-lens setup. We derive a simple formula for the filamentation distance, and confirm its agreement with the experimental results. We also observe that delaying the onset of filamentation increases the filament length.

© 2006 Optical Society of America

OCIS codes: (010.1300) Atmospheric propagation; (190.5940) Self-action effects; (190.5530) Pulse propagation and solitons; (190.7110) Ultrafast nonlinear optics

References and links

1. L. Wöste, C. Wedekind, H. Wille, P. Rairoux, B. Stein, S. Nikolov, C. Werner, S. Niedermeier, F. Ronnenberger, H. Schillinger, and R. Sauerbrey, "Femtosecond atmospheric lamp," *Laser und Optoelektronik* **29**, 51–53 (1997).
2. P. Sprangle, J.R. Peñano and B. Hafizi, "Propagation of intense short laser pulses in the atmosphere," *Phys. Rev. E* **66**, 046418, 2002.
3. G. Fibich, S. Eisenmann, B. Ilan, Y. Erlich, M. Fraenkel, Z. Henis, A.L. Gaeta, and A. Zigler, "Self-focusing distance of very high power laser pulses," *Opt. Express* **13**, 5897–5903 (2005).
4. A.L. Gaeta, "Collapsing light really shines," *Science* **301**, 54–55 (2003).
5. J. Kasparian, M. Rodriguez, G. Méjean, J. Yu, E. Salmon, H. Wille, R. Bourayou, S. Frey, Y.-B. André, A. Mysyrowicz, R. Sauerbrey, J.-P. Wolf, and L. Wöste, "White-light filaments for atmospheric analysis," *Science* **301**, 61–64 (2003).
6. A. Couairon, "Light bullets from femtosecond filamentation," *Eur. Phys. J. D.* **27**, 159–167 (2003).
7. S. Tzortzakis, L. Bergé, A. Couairon, M. Franco, B. Prade, and A. Mysyrowicz, Breakup and Fusion of Self-Guided Femtosecond Light Pulses in Air," *Phys. Rev. Lett.* **86**, 5470–5473 (2001).
8. Z. Jin, J. Zhang, M.H. Xu, X. Lu, Y.T. Li, Z.H. Wang, Z.Y. Wei, X.H. Yuan, and W. Yu, "Control of filaments induced by femtosecond laser pulses propagating in air," *Opt. Express* **13**, 10424–30 (2005).
9. R. Nuter, S. Skupin, and L. Bergé, "Chirp-induced dynamics of femtosecond filaments in air," *Opt. Lett.* **30**, 917–9 (2005).
10. G. Méchain, A. Couairon, Y.-B. André, C.D'Amico, M. Franco, B. Prade, S. Tzortzakis, A. Mysyrowicz, R. Sauerbrey, "Long-range self-channeling of infrared laser pulses in air: a new propagation regime without ionization," *App. Phys. B* **79**, 379–382 (2004).
11. G. Méchain, C.D'Amico, Y.-B. André, S. Tzortzakis, M. Franco, B. Prade, A. Mysyrowicz, A. Couairon, E. Salmon, R. Sauerbrey, "Range of plasma filaments created in air by a multi-terawatt femtosecond laser," *Opt. Commun.* **247**, 171–180 (2005).
12. V.I. Talanov, "Focusing of light in cubic media," *JETP Lett.* **11**, 199–201 (1970).

13. Q. Luo, S.A. Hosseini, W. Liu, J.F. Gravel, O.G. Kosareva, N.A. Panov, N. Aközbek, V.P. Kandidov, G. Roy, S.L. Chin, "Effect of beam diameter on the propagation of intense femtosecond laser pulses," *Appl. Phys. B* **80**, 35–38 (2005).
14. S.L. Chin, S.A. Hosseini, W. Liu, Q. Luo, F. Théberge, N. Aközbek, A. Becker, V.P. Kandidov, O.G. Kosareva, and H. Schroeder, "The propagation of powerful femtosecond laser pulses in optical media: physics, applications, and new challenges," *Can. J. Phys.* **83**, 863-905 (2005).
15. B.E.A. Saleh and M.C. Teich, *Fundamentals of photonics*, (John Wiley & sons, Inc., New York, 1991).
16. M. Mlejnek, E.M. Wright, and J.V. Moloney, "Moving-Focus Versus Self-Waveguiding Model for Long-Distance Propagation of Femtosecond Pulses in Air," *IEEE J. Quantum Electron.* **35**, 1771 (1999).
17. A. Dubietis, E. Gaižauskas, G. Tamošauskas, P. Di Trapani, "Light filaments without self-channeling," *Phys. Rev. Lett.* **92**, 253903 (2004).
18. W. Liu, Q. Luo, F. Théberge, H.L. Xu, S.A. Hosseini, S.M. Sarifi, S.L. Chin, "The influence of divergence on filament length during the propagation of intense ultra-short laser pulses," *Appl. Phys. B* **82**, 373–376 (2006).
19. A. Couairon "Filamentation length of powerful laser pulses," *Appl. Phys. B* **76**, 789–792 (2003).

1. Introduction

The possibility to send high-power ultrashort laser pulses into the atmosphere that would propagate over several kilometers [1] has sparked the interest of many researchers in nonlinear optics. As a result, atmospheric propagation of high-power lasers is currently a very active area of research, with potential applications such as remote sensing of the atmosphere using LIDAR applications and lightning control [1, 2, 3, 4, 5, 6, 7, 8]. Typically, the collapse/filamentation distance of laser pulses in air is on the order of several meters. Quite often in atmospheric applications, however, one would like to be able to delay and to control the filamentation distance, so that it would be anything from a few meters up to several kilometers. Until very recently, the only approach to achieve that was to launch negatively chirped ultrashort pulses [1, 2]. The idea behind this approach is that the increase in pulse duration due to the normal group velocity dispersion (GVD) of the air is precompensated by imparting a negative initial chirp that makes the pulse compress in time as it propagates. In this approach one can control the collapse/filamentation distance through delicate changes in the amount of negative chirping.

In this study, we show that the filamentation distance can also be increased with a defocusing lens. Our analysis of the effect of a lens on the filamentation distance is based on two key observations:

1. Prior to beam collapse, the propagation in the atmosphere is essentially determined by the Kerr nonlinearity and diffraction, as other effects (multiphoton absorption, plasma formation, Raman scattering, etc.) become important only after the pulse has collapsed. As a result, the collapse point can be calculated with the relatively simple two-dimensional, cubic Nonlinear Schrödinger model (NLS). This observation holds regardless of whether the beam collapses as a single filament or as multiple filaments.
2. The effect of a focusing/defocusing lens in the two-dimensional, cubic NLS is the same as in diffractionless, linear propagation.

Together, these two observations imply that if we denote by z_c the filamentation distance of the original beam, by z_c^F the filamentation distance of the focused/defocused beam, and by F the focal length of the lens, then z_c and z_c^F are related by the simple lens relation

$$\frac{1}{z_c^F} = \frac{1}{z_c} + \frac{1}{F}. \quad (1)$$

Recently, Jin et al. [8] demonstrated experimentally that the filamentation distance in air can be controlled with a deformable mirror. In Section 3 we show that the experimental results of [8] can be explained with relation (1). This shows, in particular, that the relatively expensive

deformable mirror effectively acts as a focusing/defocusing lens. If one uses a lens with a focal length F , however, one can only change the collapse distance from z_c to z_c^F . Hence, a continuous control can only be achieved by changing the power of the beam (in order to change z_c). Unfortunately, this requires a very delicate control over the laser power, which is hard to achieve with the Terawatts lasers that are used in atmospheric propagation. In order to overcome this difficulty, in our experimental setup we used a telescope-type double-lens system, in which the filamentation distance is controlled by changing the distance d between the two lenses. In that case, a derivation similar to that of relation (1) shows that the double-lens setup changes the filamentation distance from z_c to

$$z_c^{F_1, F_2}(d) = d + F_2 \frac{z_c(F_1 - d) - dF_1}{(F_1 + F_2)z_c + F_1F_2 - d(z_c + F_1)}, \quad (2)$$

where F_1 and F_2 are the focal lengths of the first and second lens, respectively.

In our experiments, we were able to use the double lens setup to control the filamentation distance, as well as to increase the filamentation distance in air by a factor of six (e.g., from 8 to 47 meters). We could not observe filamentation distances greater than 50m because of the size of the laboratory. Our theoretical prediction for the filamentation distance as a function of the distance between the two lenses, equation (2), is in good quantitative agreement with our experimental results.

In our experiments, we also observed that the increase in the distance of the onset of filamentation was accompanied by an increase in the filament length. A similar phenomenon was observed for negatively chirped pulses, where the delay of the onset of filamentation was accompanied by an increase in the filament length [9, 10, 11]. This similarity further suggests that a defocusing lens can be viewed as the “spatial analogue” of negative chirping.

2. Effect of a lens

The mathematical model for atmospheric propagation of intense laser pulses can be quite complex. This is due to the fact that *after* the beam has collapsed into a filament, its intensity becomes so high that, in addition to the Kerr nonlinearity and diffraction, various other nonlinear effects (e.g., nonlinear saturation, nonlinear absorption, and plasma formation) become important. Until the beam begins to collapse, however, these nonlinear effects are negligible, and the propagation is dominated by the effects of the Kerr nonlinearity and diffraction. Therefore, the pulse propagation *prior* to filamentation/collapse can be modeled by the Nonlinear Schrödinger equation (NLS), which in dimensionless variables reads

$$iA_z(z, x, y) + \nabla^2 A + |A|^2 A = 0. \quad (3)$$

Here, A is the complex amplitude of the electric field, z is the distance in the direction of propagation, normalized by twice the diffraction (Rayleigh) length $L_{\text{diff}} = k_0 r_0^2$, and x and y are the transverse coordinates measured in units of the initial beam width r_0 .

The two-dimensional cubic NLS, equation (3), has the following remarkable property, sometimes known as the *lens transformation* [12]. Let $A(z, x, y)$ be a solution of the NLS (3), let

$$L(z) = 1 - z/F, \quad (4)$$

and let

$$A^F(z, x, y) = \frac{1}{L(z)} A(\zeta, \xi, \eta) e^{i\frac{Lz}{2} \frac{x^2 + y^2}{4}},$$

where

$$\xi = \frac{x}{L(z)}, \quad \eta = \frac{y}{L(z)}, \quad \zeta(z) = \int_0^z \frac{1}{L^2}. \quad (5)$$

Then $A^F(z, x, y)$ is also an exact solution of the NLS (3). In the linear case, the lens transformation holds in all dimensions. In the case of a cubic nonlinearity, however, the lens transformation holds only in the two-dimensional case.

Since $A^F(0, x, y) = A(0, x, y)e^{-i(x^2+y^2)/4F}$ and

$$\frac{1}{\zeta} = \frac{1}{z} + \frac{1}{F}, \quad (6)$$

the lens transformation shows that the effect of a lens in diffractive propagation in a bulk Kerr medium is the same as in diffractionless, linear propagation. In particular, if $A(z, x, y)$ collapses at $z = z_c$, then $A^F(z, x, y)$ would collapse at $z = z_c^F$, where

$$\frac{1}{z_c^F} = \frac{1}{z_c} + \frac{1}{F}. \quad (7)$$

Equation (7) shows that a focusing lens ($F > 0$) accelerates the collapse, i.e., $z_c^F < z_c$, and a defocusing lens $F < 0$ delays the collapse, i.e., $z_c^F > z_c$. Moreover, it shows that in principle, with a proper choice of the lens, the beam can be made to collapse at any desired location, before or after the “original” collapse point z_c . We emphasize that the lens transformation models the effect of an infinitely thin lens. The finite width of lenses used in experiments, as well as their nonlinear properties, can lead to deviations from the predictions of the lens transformation.

It is worth noting that the “original” input beam does not have to be collimated, since in the lens transformation we did not assume that the input beam $A(0, x, y)$ is collimated. It is also worth noting that the lens transformation shows that *the addition of a thin lens does not change the filamentation pattern in the NLS (3)*. Specifically, if the “original” beam breaks into multiple filaments before it collapses, the focused beam would break into the same number of filaments.

The above statements have been proved under two conditions. The first condition is that the lens is *thin*. Thus, a “thick” lens may affect the filamentation pattern by introducing small-scale aberrations to the beam profile. The second condition is that multiple filamentation occurs when the propagation dynamics is still governed by the NLS (3). This is indeed the case for beams whose power is of the order of $100P_{cr}$ or more, since in this high-power regime multiple filamentation occurs just before the beam collapses [3]. However, at “lower” powers, multiple filamentation occurs after the collapse is arrested, i.e., when the NLS model, hence the lens transformation, are not valid. In that case, the lens may affect the filamentation pattern.

Since in atmospheric propagation we would like to delay the onset of filamentation, from now on we will focus on the case of a defocusing lens. Our results, however, are also applicable to the case of a focusing lens.

The effect of a defocusing lens on the collapse distance, as given by equation (7), is illustrated in Fig. 1. When the beam is collimated ($-F = \infty$), the beam collapses at z_c . As $-F$ decreases from $-F = \infty$ to $-F = z_c$, the collapse distance increases from z_c to infinity. When $-F < z_c$, the value of z_c^F becomes negative, indicating that there is no collapse. In other words, a defocusing lens whose “imaginary” focus is shorter than the distance to the blowup point without the lens will prevent the collapse.

In Fig. 2 we show the effect of a defocusing lens on the propagation of a Gaussian beam with input power $P = 9P_{cr}$. When the beam is collimated ($-F = \infty$), it self-focuses until it collapses at the dimensionless distance of $z_c = 0.0423$. When $-F = 1.18z_c$, i.e., slightly above z_c , the beam initially diffracts (due to the lens) until $z/z_c \approx 2$ and later collapses at $z_c^F/z_c \approx 6.5$. When $-F = 1.0034z_c$, the beam initially diffracts due to the lens until $z/z_c \approx 20$, then propagates at a defocused stage until $z/z_c \approx 110$ and finally collapses at $z_c^F/z_c \approx 300$. When $-F = 0.9975z_c$, i.e., slightly below z_c , the defocusing lens is stronger than the Kerr nonlinearity, hence the pulse simply diffracts.

Ideally, in order to achieve long-distance atmospheric propagation, we would like the propagation to be as in Fig. 2C. Here, the collapse distance increased by a factor of ≈ 235 , compared with the collapse distance in the absence of the defocusing lens. Moreover, during most of the propagation, the beam intensity is substantially lower (by a factor of ≈ 55) than its initial intensity. Hence, the effects of nonlinear absorption, as well as of any other nonlinear mechanism, are minimized. In that case, the justification for using the NLS model (3) until the onset of filamentation is even stronger.

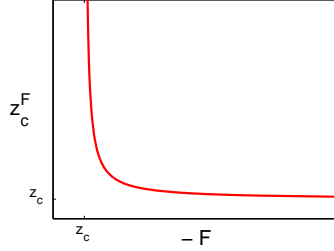


Fig. 1. Control of the location of the blowup point z_c^F with a defocusing length with focal length F .

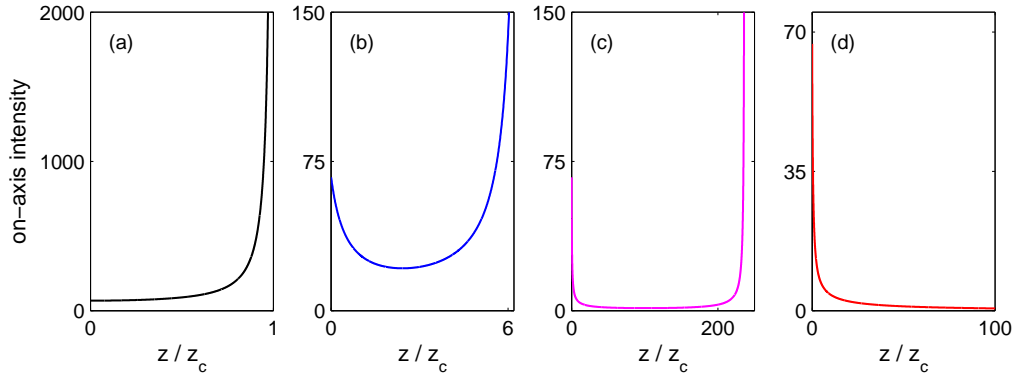


Fig. 2. Dynamics of the on-axis intensity of the solution of the NLS (3) with various defocusing lenses. (a) $F = -\infty$; (b) $-F = 1.18z_c$; (c) $-F = 1.0034z_c$; (d) $-F = 0.9975z_c$.

3. Deformable mirror experiment

In [8], Jin et al. showed that the filamentation distance in air can be controlled by changing the beam divergence angle θ with a deformable mirror and also by changing the input power. In Figure 8 in that study, the authors fitted the results of one set of experiments (with input power $P = 300GW$) with the following approximation for the filamentation distance, which in dimensionless variables reads as

$$z_c^{Jm}(\theta) \sim \frac{\sqrt{2(p-1) + r_m^2 \tan^2 \theta} + \tan \theta}{2(p-1) - \tan^2 \theta}, \quad (8)$$

where $p = P/P_{\text{cr}}$ is the fractional input power, r_m is the dimensionless focal spot size, and a positive/negative value of θ corresponds to a diverging/converging beam. There are, however, several problems with the analytical approximation (8). For one thing, according to equation (8), in the case of a collimated beam,

$$z_c^{\text{Jin}}(\theta = 0) \sim \frac{1}{\sqrt{2(p-1)}}.$$

This square-root dependence is indeed correct for input powers $\ll 100P_{\text{cr}}$. However, at input powers above $100P_{\text{cr}}$, which was the case in that experiment, the collapse distance should scale as $1/P$, see [3]. The reason equation (8) provided a good fit to the experimental data is because the value of P used in the fit was 40GW (the measured value of the integrated laser pulse in the filament) rather than the input power of 300GW . Therefore, the second drawback of this analytical approach is that it requires measuring the filament spot size and the integrated power in the filament.

We now show that the experimental results of Jin et al. can be explained with equation (7). Note that this approach does not require knowledge of the filament spot size, nor of the integrated power in the filament. Instead, it uses the value of z_c , the filamentation distance in the absence of the deformable mirror, whose value as a function of the input power P can either be measured “once and for all”, or calculated numerically.

Since the divergence angle θ is related to the focal distance through

$$\tan \theta = -\frac{r_0}{F},$$

rewriting equation (7) in terms of θ gives

$$\frac{1}{z_c(\theta)} = \frac{-1}{r_0} \tan \theta + \frac{1}{z_c}. \quad (9)$$

In Fig. 3 we present the data taken from Fig. 8 of Ref. [8] for three different power levels. Motivated by equation (9), we plot $1/z_c(\theta)$ as a function of $\tan \theta$, and indeed observe that

1. For each power level, the results are on a straight line.
2. All three lines have essentially the same slope.

These two observations are in a remarkable agreement with the theoretical model (9). A linear fit of the data, with $1/r_0$ and $1/z_c$ being the fitting parameters, gives values of $r_0 = 10.7\text{mm}$, 8.7mm and 9.5mm for the cases of $P = 350\text{GW}$, 400GW and 450GW , respectively. The fact that the three values of r_0 are in good agreement with each other is consistent with equation (9), since varying the input power P affects only the collapse distance z_c . These three values are also in reasonable agreement with the value of $r_0 = 15\text{mm}$ reported in [8]; the minor difference is probably due to using different definitions of the beam width.

4. Double Lens setup

The results of Section 3 show that the effect of the deformable mirror is equivalent to that of a defocusing lens. Therefore, the filamentation distance can be controlled with a simple defocusing lens, rather than with the more sophisticated (and more expensive) deformable mirror. A defocusing lens also has a higher damage threshold than a deformable mirror, which can be an advantage considering the high powers needed for atmospheric propagation. However, if we replace the deformable mirror with a single lens with a fixed focal length F , we would face new

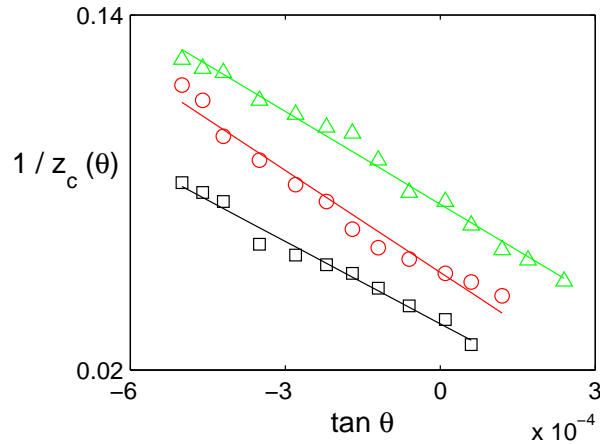


Fig. 3. Experimental data extracted from Fig. 8 in [8]. Filamentation distance in air as a function of divergence angle θ . Input power is $P = 300\text{GW}$ (black, squares), $P = 350\text{GW}$ (red, circles), and $P = 400\text{GW}$ (green, triangles).

obstacles. Indeed, we have seen that in order to achieve a considerable delay, the focal length should be slightly larger than z_c . Since the typical filamentation distance z_c in air is 5–15m, the focal length of the defocusing lens should be in that range, in order to achieve a significant delay. Such defocusing lenses are, however, less common. Moreover, with a fixed focal length F , one could only achieve a continuous control of the location by varying the input power. When $-F$ is slightly larger than z_c , however, the filamentation distance is extremely sensitive to small variations in the difference between z_c and $-F$ (compare, e.g., Fig 2(b) with Fig 2(c)). Therefore, the required level of control over the laser power would be beyond what could be expected from lasers operating at the high powers needed for atmospheric propagation.

We overcome the above difficulties as follows. We reduce the strong defocusing of the lens by adding a second, weaker focusing lens. This way, the effective lensing obtained by the double lens system is weaker than of a single defocusing lens. More importantly, for a fixed laser power, we obtain continuous control of the location of the filamentation distance by continuously changing the distance between the two lenses. Hence, the double lens system acts as an adjustable lens. We note that a similar double lens setup was used by Luo *et al.* in [13, 14]. In that study, however, the goal of the telescope was to control the width of the beam and not the filamentation distance.

4.1. Analysis

In our experimental setup described below, a defocusing lens with focal length $F_1 < 0$ is placed at $z = 0$, and a defocusing lens with focal length $F_2 > 0$ is placed at $z = d$. The defocusing lens was chosen to be stronger than the focusing lens ($-F_1 < F_2$), in order for the effective lensing to be weakly defocusing. We determined which lens should be placed first as follows. By equation (4), the beam width at the second lens changes by a factor of

$$L(z = d) = (1 - d/F_1) \quad (10)$$

relative to its initial width. As a result, the effective Rayleigh length $L_{\text{diff}} = k_o r_0^2$ changes by a factor of $(1 - d/F_1)^2$. Therefore, we can delay the onset of collapse by increasing the effective Rayleigh length, which would be achieved by placing the defocusing lens first and the focusing

lens second. Clearly, if one is interested in accelerating the collapse, the focusing lens should be placed first.

We now analyze the effect of a double lens setup with two successive applications of the lens transformation. The effect of the first lens is given by

$$\frac{1}{z^{F_1}} = \frac{1}{z} + \frac{1}{F_1}, \quad 0 < z < d.$$

Similarly, the effect of the second lens is given by

$$\frac{1}{z^{F_1, F_2} - d} = \frac{1}{z^{F_1} - d} + \frac{1}{F_2}, \quad d < z.$$

Eliminating z^{F_1} gives

$$z^{F_1, F_2} = d + F_2 \frac{z F_1 - d z - d F_1}{(F_1 + F_2 - d) z + F_1 F_2 - d F_1}. \quad (11)$$

This equation is the same as the imaging equations for the two lenses in linear geometrical optics. Indeed, by replacing $-z \rightarrow u$ and $z^{F_1, F_2} \rightarrow v$, we get that

$$v = d - F_2 \frac{(F_1 - d)u + d F_1}{(d - F_1 - F_2) u + F_1 F_2 - d F_1}.$$

The relation between u and v cannot be written simply as a (thin) lens imaging relation but rather it represents a *thick lens* imaging relation. In such a relation there is a difference between the forward focal length ($u \rightarrow \infty$) and backward focus length ($v \rightarrow \infty$) [15].

If, as before, we denote by z_c the filamentation distance in the absence of the double-lens setup, then Eq. (12) shows that the double lens setup changes the filamentation distance to

$$z_c^{F_1, F_2} = d + F_2 \frac{z_c(F_1 - d) - d F_1}{(F_1 + F_2)z_c + F_1 F_2 - d(z_c + F_1)}. \quad (12)$$

We emphasize that Eq. (12) is an exact relation for the collapse point in the NLS model (3). The remarkable resemblance between the results for the NLS and for linear geometrical optics is due to the lens transformation property of the NLS (see Section 2).

The denominator in (12) vanishes at

$$d_c = F_1 + F_2 - \frac{F_1^2}{F_1 + z_c}.$$

We note that in the absence of the double lens, the filamentation distance z_c is of the order of several meters, whereas F_1 , F_2 and d are below $0.5m$. Therefore,

$$F_1, F_2, d \ll z_c.$$

Therefore, for $d \approx d_c$, equation (12) can be approximated with

$$z_c^{F_1, F_2} \approx d_c - \underbrace{F_2 \frac{z_c(d_c - F_1)}{z_c + F_1}}_{>0} \frac{1}{(d_c - d)}.$$

We thus see that when d is slightly below d_c , the value of $z_c^{F_1, F_2}$ is negative (i.e., there is no collapse). In other words, the double lens setup is defocusing stronger than the Kerr nonlinearity. This case is thus similar to that of a defocusing lens with $-F < z_c$ (see Section 2).

When d is slightly above d_c , the collapse point is mapped to “near infinity”. As d increases from d_c , the collapse point decreases from $z_c^{F_1, F_2} = +\infty$. Because of the $d_c - d$ term in the denominator, the changes in $z_c^{F_1, F_2}$ are very fast (see Figure 4). For example, when $d = d_0 = F_1 + F_2$, the collapse distance is given by

$$z_c^{F_1, F_2}(d_0) = F_1 + 2F_2 + \frac{F_2^2(z_c + F_1)}{F_1^2} \approx \frac{F_2^2}{F_1^2} z_c.$$

The change of z_c by a factor of F_2^2/F_1^2 is due to the effective change of the beam width by a factor of, see equation (10),

$$L(z = d_0) = \left(1 - \frac{F_1 + F_2}{F_1}\right) = -\frac{F_2}{F_1} = \left|\frac{F_2}{F_1}\right|,$$

which changes the Rayleigh length by F_2^2/F_1^2 . Indeed, when $d = d_0$ the lenses are aligned as in a telescope, so that if the input beam is collimated, the beam emerging from the double lens setup will also be collimated. Hence, in that case the double lens setup changes the value of z_c “only” by changing the effective Rayleigh distance.

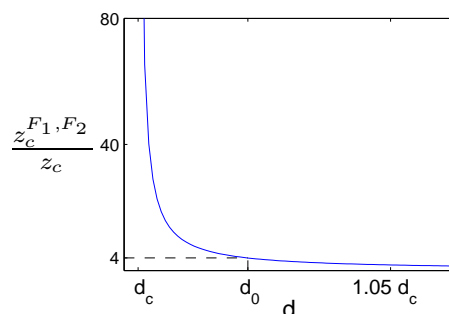


Fig. 4. The filamentation distance as a function of the distance between the two lenses (d) for the double lens system with $F_1 = -0.5F_2 < 0$.

4.2. Experimental setup and results

The experiments were conducted using a 55fs laser system at 800nm, capable of delivering up to 5TW. The beam radius was $r_0 \approx 20\text{mm}$ corresponding to initial intensity up to $10^{12}\text{W}/\text{cm}^2$. The double-lens consisted of a defocusing lens ($F_1 = -0.252\text{m}$), which was placed at the compressor exit, followed by a focusing lens ($F_2 = 0.504\text{m}$), whose distance d from the first lens was continuously varied (see Fig 5). After passing through the telescopic system, the laser pulse propagated in air ($P_{\text{cr}} \approx 3\text{GW}$) within the laboratory. The existence of a filament was determined with a Polyvinyl Chloride (PVC) target, whose damage threshold for 55fs pulses is $\approx 10^{13}\text{W}/\text{cm}^2$. This damage threshold is high enough so the beam without filamentation is not producing any damage. The collapse distance was defined as the shortest propagation distance at which the laser beam could create a visible damage to the PVC.

In our experiments, we measured the collapse distance and the filament length in air, as a function of the distance between the two lenses of the telescope. In these experiments, we always observed multiple filaments at the initial collapse point, which is typical for input powers that are above $100P_{\text{cr}}$ [3]. The presence of the telescope did not seem to change the number of filaments at the initial collapse point, in agreement with our analysis in Section 2.

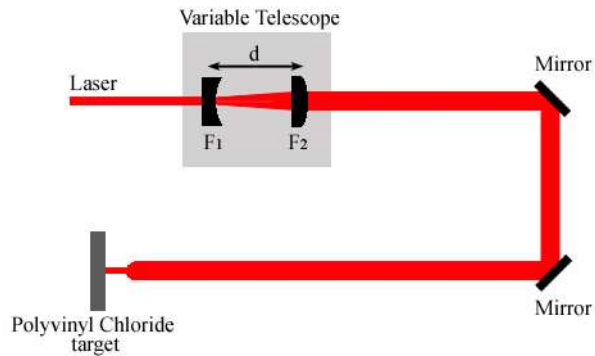


Fig. 5. Experimental setup of the double-lens system and filamentation distance measurement.

In Fig. 6 we show the filamentation distance as a function of the distance between the lenses d . As predicted by our analysis:

1. The filamentation distance decreases as the distance between the lenses increases.
2. The filamentation distance is sensitive to small changes in the distance between the lenses.
3. Setting a stronger defocusing lens, followed up by a weaker focusing lens, can result in a considerable increase in the filamentation distance. For example, In Fig. 6(a) the collapse distance increases from $z_c = 11m$ up to $z_c^{F_1, F_2} = 53m$; in Fig. 6(b) the collapse distance increases from $z_c = 8.2m$ up to $z_c^{F_1, F_2} = 47m$. Observation of filamentation distances greater than 50m was not possible because of the length of our laboratory.

Moreover, the results in Figure 6 show a convincing quantitative agreement between the theoretical prediction, Eq. (12), and the experimental results. The $\approx 1mm$ deviations in the values of d between the experimental data and the theoretical prediction are well within the experimental errors, considering the shot-to-shot fluctuations in the laser power and the finite thickness (7mm and 11mm) of the two lenses.

4.3. Filament length

We also measured the position where the filament “ended”, i.e., where the laser beam ceased to create a visible damage to the PVC target. In Figure 7 we show the filament length, defined as the distance between the earliest and latest distances where the filament is observed, as a function of the filamentation distance. One can see that *the filament length increases with the filamentation distance*.

We now discuss some possible explanations for the increase in the filament length. The filament depends on the power of the filament and of the surrounding “energy reservoir” [16, 17]

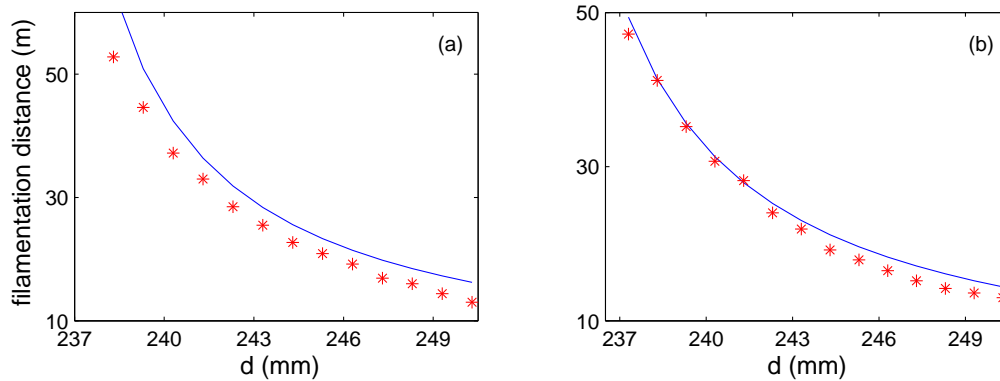


Fig. 6. Experimental data (stars) and theoretical prediction (solid line) of the filamentation distance as a function of the distance between the lenses. (a) $P \approx 660P_c$ and $z_c = 11m$; (b) $P \approx 780P_c$ and $z_c = 8.2m$.

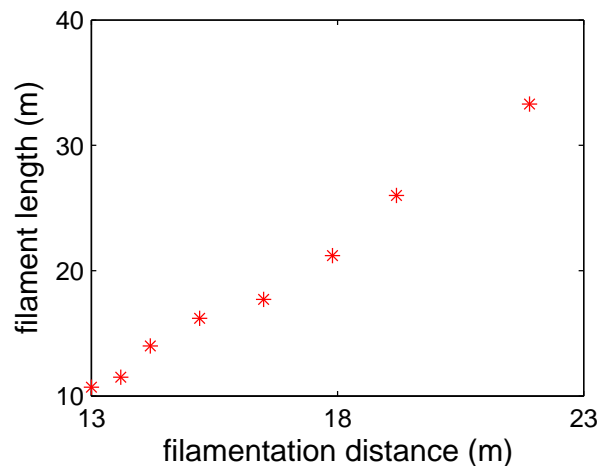


Fig. 7. Filament length as a function of the filamentation distance, for the experimental data of Fig. 6 (b).

at the onset of filamentation. This power, however, is unaffected by the change of the filamentation distance. Indeed, for the distances involved in our experiments ($< 50m$), linear losses in atmospheric propagation are truly negligible. Moreover, when linear losses are important, then the pulse power at the onset of filamentation is *lower* for a longer propagation distance, hence the filament length *decreases*. Similarly, nonlinear losses do not affect the beam power at the onset of collapse because they become important only when the beam intensity increases substantially, i.e., after the collapse. The beam power may also decrease with propagation due to the temporal broadening effect of the group velocity dispersion. This effect, however, becomes important only after propagation distances of several hundreds of meters. We thus see that in our experiment, the beam power at the onset of collapse is independent of the filamentation distance. Hence, it cannot explain the increase of the filament length.

The length of a single filament depends also on the convergence angle at the onset of col-

lapse [18]. Using the lens transformation, it can be shown that a stronger defocusing lens does not only delay the onset of collapse/filamentation, but also lowers the convergence angle there. It is quite likely, therefore, that this change in the convergence angle leads to an increase in the filament length. This explanation is also valid when the beam breaks into several well-separated filaments. If, however, the filaments are close to each other, the change in the convergence angle may affect the interaction between the filaments, and, as a result, the total filament length. In that case, the effect of changing the convergence angle is less clear.

We note that a similar increase in the filament length with the filamentation distance was observed for negatively chirped pulses [10, 11]. However, unlike a defocusing lens that affects only the spatial phase distribution, chirping affects both the temporal phase distribution and the pulse duration (hence, the beam power). Nuter *et al.* [9] showed that both positive and negative chirping increase the filamentation distance. However, negative chirping increased the filament length whereas positive chirping reduced it. Moreover, they observed that negative chirping increased the filament length and positive chirping reduced it even if the pulse duration remains constant and only the temporal phase distribution is “chirped”. Since the change in the pulse duration is independent of the sign of the chirping, these results suggest that the change of the filament length in that study was mainly due to the effect of chirping on the temporal phase distribution. In that case, a defocusing lens can be viewed as the “spatial analogue” of negative chirping. In another study, however, Couairon [19] used an energy depletion analysis to show that for non-chirped pulses, the pulse duration affects the filament length. Therefore, the increase of the filament length with negative chirping may be due to the combined effects of the increase of pulse duration and the change of the temporal phase distribution.

5. Conclusions

In this study we showed experimentally that the filamentation distance in air can be continuously controlled with a double lens setup. We also derived a simple formula for the dependence of the filamentation distance on the distance between the two lenses, and showed that it is in good agreement with measurements of the filamentation distance in air. We believe that the combination of a simple control tool (two lenses) with an accurate theoretical formula for the filamentation distance will provide a useful tool for filamentation control in both current and future atmospheric applications.

One advantage of the double lens setup is that it can be used with pulses of any duration, and not just with ultrashort pulses. Since the limiting quantity in self-focusing is the pulse power, the possibility to work with longer pulses means that the filament can contain more energy.

In our model we neglected temporal effects, which allowed for a considerable simplification in the analysis. However, while nonlinear temporal effects (plasma formation, Raman etc.) can be neglected so long as the pulse does not begin to collapse, linear temporal effects, namely, group velocity dispersion (GVD), may become important for propagation distances of the orders of kilometers. Note, however, that in that case, if needed, the effect of GVD can be minimized by working with longer pulses.

Acknowledgments

The research of S. Eisenmann, Y. Katzir and A. Zigler was partially supported by BSF grant 2002-155.